Journal of Structural Geology, Vol. 6, No. 1/2, pp. 167 to 182, 1984
Printed in Great Britain

0191-8141/84 $03.00 + 0.00
Pergamon Press Ltd.

Deformation microfabric development in chalcopyrite in fault zones, Mt. Lyell, Tasmania

S. F. Cox and M. A. Etheridge*

Department of Earth Sciences, Monash University, Clayton, Victoria 3168, Australia

(*Accepted in revised form* 11 *July* 1983)

Abstract—Deformation of chalcopyrite ($CuFeS_2$) under low-grade metamorphic conditions within fault zones in the Mt. Lyell area of western Tasmania (Australia) has occurred dominantly by dislocation flow processes. Elongate grain fabrics and well-developed crystallographic preferred orientations have developed by $\{112\}\langle 1\bar{1}0\rangle$/$\langle\bar{2}01\rangle$ dislocation glide. However, the presence of recovered dislocation substructures indicate that dislocation climb has also been important.

At strains greater than about 30% shortening, strain induced grain boundary migration and deformation band boundary migration are associated with the initial development of a dynamically recrystallized microstructure. However, subgrain rotation and subgrain coalescence mechanisms of recrystallization appear to have been important following the initial dynamic recrystallization of the original grain boundary regions of host grains. In some cases significant grain growth by twin coalescence has followed new grain nucleation.

Deformation by $\{112\}$ twin glide, and to a lesser extent brittle failure mechanisms, has been significant in some fault zones. The twin glide deformation mechanism is interpreted to have operated in a higher deviatoric stress environment and possibly lower temperature regime than that in which dislocation glide and climb have been the dominant mechanisms. Brittle failure may have occurred in a still higher deviatoric stress regime, a lower temperature regime, or perhaps by hydraulic fracture during periods of local high fluid pressure in the fault zones.

INTRODUCTION

In recent years detailed microstructural analysis and experimental deformation studies have contributed considerably to our understanding of the behaviour of some sulphide minerals during natural deformation. There have been several experimental studies of the strength and mechanical behaviour of chalcopyrite in particular (Lang 1968, Atkinson 1974, Kelly & Clark 1975, Roscoe 1975) at low to moderate temperatures and relatively high differential stresses. However there has been little systematic and detailed documentation of deformation microfabrics developed in naturally deformed chalcopyrite.

This paper describes and discusses a variety of deformation microstructures developed in chalcopyrite deformed under low-grade metamorphic conditions. In the Mt. Lyell area of western Tasmania (Australia) movement along fault zones containing massive chalcopyrite vein deposits has produced a range of deformation microstructures. These microstructures reflect the operation of different deformation mechanisms in various temperature, pressure, and deviatoric stress regimes, as well as over a range of total strains.

The microstructures of four suites of samples have been studied in detail.

(1) In a narrow ductile shear zone, a complete progressive microstructural transition is exposed, with increasing strain from little deformed chalcopyrite to chalcopyrite mylonites. The chalcopyrite microstructures are very similar to those of many silicate and carbonate mylonites, and metals and ceramics deformed to high strain.

(2) Coarser-grained chalcopyrite mylonites from various other shear zones illustrate well the details of intragranular deformation microstructures, and the microstructures developed during dynamic recrystallization.

(3) The third suite of mylonites to be discussed illustrates the microstructural change involved in grain growth following primary recrystallization.

(4) Finally, we briefly examine weakly strained specimens in which deformation has occurred dominantly by twin glide mechanisms and to a lesser extent by brittle failure processes.

Geological setting of the vein deposits

The chalcopyrite discussed in this study occurs as deformed vein deposits within and adjacent to fault zones in the Cambrian volcanic-hosted disseminated pyrite–chalcopyrite ore bodies of the Mt. Lyell area (Reid 1975, Cox 1981). The fault zones and associated vein deposits developed during regional middle Devonian deformation and low-grade metamorphism. Peak metamorphic temperatures were around 300–350°C, and confining pressures were probably around 200 MPa (Cox 1981). On the scale of several metres, the distribution of chalcopyrite veins and lenses within the fault zones is erratic, however chalcopyrite is not developed within the fault zones outside areas containing the Cambrian disseminated chalcopyrite mineralization. The chalcopyrite lenses and veins appear to have developed late during regional deformation by deposition of chalcopyrite in opening fractures from metamorphic fluids rich in locally derived copper dissolved during cleavage development in the surrounding disseminated Fe–Cu ore bodies. Chalcopyrite pods and lenses within fault zones range up to several cubic metres in volume, and consist of generally coarse-grained chal-

*Present address: Bureau of Mineral Resources, P.O. Box 378, Canberra City, A.C.T. 2601, Australia.

copyrite with only minor amounts of pyrite, quartz, siderite and chlorite.

Methods of examination

As chalcopyrite is a tetragonal opaque phase which is essentially isotropic in incident light, reflection optical microscopy has been performed on etched polished sections. Three etching techniques have proved useful during optical microstructural analysis. The H_2O_2/NH_4OH solutions described by Richards (1966), Kelly & Clark (1975) and Roscoe (1975) give a colourful surface tarnish etch which is sensitive to crystal lattice orientation, and thus provide information on the geometry of grain and twin boundaries as well as intragranular lattice misorientations. Electrolytic etching of specimens in a saturated chromic acid solution (Atkinson 1974) dissolves chalcopyrite preferentially along grain boundaries and twin boundaries. Some polishing of the specimen surface may also be achieved with this technique.

Etching of subgrain boundaries as well as grain and twin boundaries may be achieved by electrolytic action using a glacial acetic acid solution. The best results are achieved if the specimen is first prepared by careful mechanical polishing, and given a pre-treatment electrolytic polish and weak etch in saturated chromic acid. For the acetic acid etch a gold sheet, held about one millimetre above the specimen surface, is used as an anode. Voltages of about 5–15 V are most suitable for etching times of about five to ten seconds. Ultrasonic cleaning and rinsing in concentrated nitric acid helps to remove any surface discolouration.

Crystallographic preferred orientation studies were performed in the reflection mode on a Siemens X-ray texture goniometer using polished thick sections. Some transmission electron microscopy (TEM) was carried out at 100 kV on thin crushed fragments of chalcopyrite. The usual argon ion beam bombardment techniques for thinning specimens proved unsatisfactory due to serious ion beam damage and cracking of specimens.

Previous studies of deformation microstructures in chalcopyrite

Amongst the earliest studies of deformation microstructures in naturally deformed chalcopyrite were those of Korn (1933), Shadlun (1953), Ramdohr (1969) and Richards (1966). Such studies clearly recognized intragranular fracturing, translation glide, deformation twinning and recrystallization.

Experimental studies on chalcopyrite have shed some light on both the conditions and processes that give rise to various microfabrics. Early studies such as those of Mügge (1920), Buerger (1928), Newhouse & Flaherty (1930), Cherviakovski (1952) and Shadlun (1953) were conducted at room temperature and high pressures. Cataclasis was the dominant deformation mechanism, but translation glide and mechanical twinning were also demonstrated. A group of intrusion experiments (Roberts 1965, Krishnamurthy 1967, Gill 1969) demonstrated increased ductility in chalcopyrite with increasing temperature. Above about 500°C chalcopyrite was found to deform and recrystallize rapidly but the flow mechanisms were not investigated.

More recent experimental studies have provided quantitative results on the strength and mechanical behaviour of chalcopyrite. Lang (1968) found that chalcopyrite deformed plastically at room temperature under confining pressures of 100 MPa or more. Preferred orientations were detectable after several per cent shortening, and were consistent with $\{112\}\langle 1\bar{1}0\rangle/\langle 0\bar{2}1\rangle$ glide. Studies at elevated temperatures (Atkinson 1974, Kelly & Clark 1975, Roscoe 1975) indicated that dislocation glide and twin glide occur in chalcopyrite at confining pressures greater than 100 MPa, and at temperatures of 200–500°C in the strain-rate regime of 10^{-4} s^{-1}–10^{-6} s^{-1}. At 300°C differential stresses around 100 MPa give steady-state flow at about 10^{-5} s^{-1}. Roscoe (1975) reported that at temperatures greater than 250°C and strain rates less than 10^{-5} s^{-1}, experimentally deformed chalcopyrite shows evidence of dynamic recovery. At the low strains attained in experimental studies to date dynamic recrystallization has not been recorded.

MICROFABRICS DEVELOPED DURING DISLOCATION FLOW DEFORMATION

Relationship between strain and microstructure in a narrow shear zone

Chalcopyrite within many fault zones at Mt. Lyell displays a variety of microstructures ranging from weakly deformed subequant grain shapes to very elongate microstructures, and in some instances partly to completely recrystallized grain aggregates. The range of microstructures is typical of that exhibited by many minerals and other materials deformed by dislocation flow mechanisms.

In one example of a narrow (2 cm) ductile simple shear zone within a small chalcopyrite lens, the relationship between strain and microstructure may be established as there is a progressive increase in strain from the margin to the centre of the shear zone. The least deformed chalcopyrite on the boundary of the shear zone forms a nearly polygonal grain aggregate, the average grain size of which is 200 μm. Grain boundaries are straight to gently curved or slightly irregular. Some grains have wide parallel-sided twins which extend right across grains or have blunt or stepped terminations. The habit is typical of growth twins, with composition planes {110}, {102} and {112} (Deer *et al.* 1969, p. 453).

With increasing strain away from the margin of the shear zone, grains become elongate and define a foliation at an angle to the shear zone boundary. The angle, θ, between the foliation plane and the shear zone boundary decreases from the boundary to the centre of the shear zone (Fig. 1a). Assuming simple shearing defor-

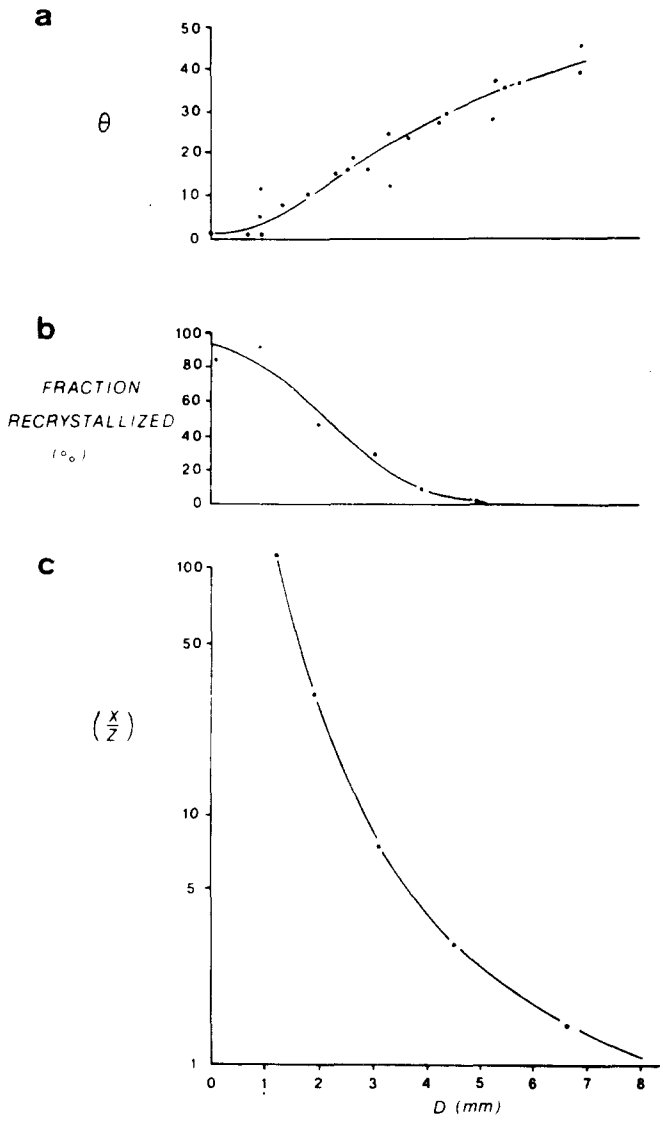

Fig. 1. (a) Angle (θ) of the grain elongation to the shear plane, plotted as a function of distance from the centre of the shear zone. (b) Abundance of recrystallized fraction as a function of distance from the centre of the shear zone. (c) Ratio of major to minor axes of the strain ellipsoid as a function of distance from the centre of the shear zone.

mation at constant volume, it is possible from a consideration of the geometry of the foliation surface to determine the strain associated with the progressive modification of the microstructures (Ramsay 1967, p. 85). Extensive modification of deformed grain shapes due to grain boundary migration and recrystallization, especially at moderate to high strains, precludes strain determination by measurement of grain shapes.

The simple shear model requires for a strain ellipsoid having principal axes X, Y and Z ($X \geq Y \geq Z$) that (1) Y is invariant, and (2) that the grain-shape foliation has formed perpendicular to the total principal shortening direction. Thus variations in the orientation of the foliation represent variations in the finite strain trajectories of the XY plane. The latter criterion is satisfied if the undeformed grains are nearly circular in cross-section; the initial polygonal grain shapes are an excellent approximation to this condition.

Ramsay (1967, p. 85) has shown that for simple shear deformation

$$\frac{X^2}{Z^2} = \frac{\gamma^2 + 2 + \gamma\sqrt{\gamma^2 + 4}}{\gamma^2 + 2 - \gamma\sqrt{\gamma^2 + 4}}$$

where γ is the shear strain, and $\tan 2\theta = 2/\gamma$. Using the above relations, X/Z values have been calculated as a function of distance from the centre of the shear zone (Fig. 1c).

With increasing strain below about 30% shortening the originally polygonal grains become progressively more elongate, growth twins become bent, and both subgrains and deformation bands develop (Figs. 2a & b). Grain boundaries and some twin boundaries also become irregularly lobate. At about 30% shortening the grain elongation foliation is quite strongly developed and the very lobate grain boundaries contain a few small (10–20 μm) equidimensional to irregularly shaped recrystallized grains (Fig. 2c).

At higher strains the abundance of small recrystallized grains increases rapidly at the expense of the large deformed elongate grains (Fig. 1b). Recrystallization occurs initially along grain boundaries, to a lesser extent along deformation band boundaries, and only to a minor extent along twin boundaries. Near the centre of the shear zone, where strains are in excess of 90% shortening, the chalcopyrite is almost entirely recrystallized, and forms an aggregate of fine-grained (<30 μm) equidimensional to slightly elongate grains with straight to gently curved grain boundaries and abundant tabular growth twins (Fig. 2d). The recrystallized grain size is approximately constant and independent of strain within the shear zone.

Relict large deformed grains form less than 10% of the aggregate at the centre of the shear zone. Their long axes measure up to 500 μm, and aspect ratios in the XZ section are typically in excess of 10:1. However the (X/Z) value of the strain ellipsoid near the centre of the shear zone is in excess of 200. Thus the shape of the relict deformed and partly recrystallized grains seriously underestimates the true strain in this part of the shear zone.

Microfabrics in unrecrystallized chalcopyrite mylonites

In most shear zones within chalcopyrite lenses there is not a simple progressive microstructural transition from the margin to the centre of the shear zone. This is due to the presence of strain discontinuities within shear zones and the discontinuous lenticular nature of chalcopyrite pods within fault zones. Much of the deformed chalcopyrite is significantly coarser grained than the previously described example, but displays an essentially similar progression of microstructures with increasing strain. It more clearly illustrates some aspects of the development of deformation microfabrics in chalcopyrite, which may also be pertinent to a wider range of materials.

At strains prior to the onset of recrystallization, coarse, and elongate deformed grains typically contain abundant deformation bands and equant to elongate subgrains (Figs. 3a–c). Deformation bands are typically subparallel to the bulk grain elongation, though in some

cases two intersecting sets are present (Fig. 3c). TEM reveals a generally low unbound dislocation density, with subgrain boundaries being defined by well-ordered dislocation arrays (Fig. 3d). This type of substructure is typical of dynamic recovery during dislocation creep in various metals (Richardson *et al.* 1966, Jonas *et al.* 1968, Takeuchi & Argon 1976) and silicates (White 1977, Kohlstedt & Weathers 1980, Zeuch 1980).

Subgrain boundaries can be irregularly shaped and bound equant to elongate subgrains, but in many cases subgrains tend to have equant to elongate blocky shapes with one or two sets of opposite sides nearly parallel and controlled by crystallographic orientation (Fig. 4). Subgrain boundaries in some cases meet at triple junctions, but they can also meet at irregular angles. Sub-boundary T-junctions are particularly common where boundaries have a marked crystallographic control. Such deformation substructures are typical of many materials deformed at high homologous temperatures by dislocation creep mechanisms (Poirier 1972, Takeuchi & Argon 1976).

Long etching periods reveal that within 'first-order' subgrains such as illustrated in Fig. 4 further dislocation walls are developed. These boundaries are more weakly etched, and in some cases they gradually die out along their length. Some of these sub-boundaries have a significantly larger etch pit separation than the main sub-boundaries, and hence probably a lower misorientation across the boundary. Such boundaries can be either irregularly oriented or crystallographically controlled, and enclose subgrains which are commonly an order of magnitude smaller than those enclosed by the higher misorientation boundaries. Such subgrain-in-subgrain structures are similar to those described in quartz mylonites (White 1979).

An example of relatively coarse irregularly shaped to elongate subgrains with deeply etched boundaries enclosing more weakly etched and closer spaced sub-boundaries is shown in Fig. 5(a). Less well-developed sub-boundaries within subgrains may also be seen in some areas illustrated in Fig. 4. Figures 4 and 5 also illustrate the variability of subgrain sizes and shapes over small areas within deformed grains. The subgrain structure in many grains is very heterogeneous, particularly adjacent to grain boundaries and deformation band boundaries. Some grains exhibit a rough core and mantle structure (White 1976), but this is not usual. Deformation band boundaries are associated with sub-planar domains of elongate subgrains having dimensions much smaller than adjacent subgrains (Fig. 5b). Correlation of changes in etch colours and the bending of deformation twins with subgrain boundary distribution suggests that, as in NaCl (Poirier 1972), rapid lattice misorientation occurs across sub-planar domains consisting of bundles of anastomosing to subparallel and closely spaced subgrain boundaries.

The elongate unrecrystallized chalcopyrite mylonites typically have a well-developed crystallographic preferred orientation (Fig. 6) which is approximately a single crystal orientation with a {112} plane close to the grain elongation foliation, and a $\langle 1\bar{1}0\rangle/\langle\bar{2}01\rangle$ direction subparallel to the grain elongation lineation.

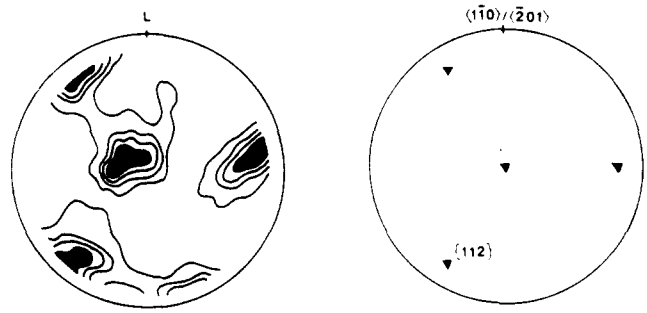

Fig. 6. {112} pole figure for coarse, deformed but unrecrystallized, chalcopyrite mylonite. Contour intervals at 1, 2, 3 and 4 times uniform. The plane of the grain elongation foliation is parallel to the projection plane, and the grain elongation lineation is parallel to L. At right the corresponding single crystal {112} distribution is shown, with a {112} plane parallel to the projection plane, and a $\langle 1\bar{1}0\rangle/\langle\bar{2}01\rangle$ direction parallel to L.

Microfabrics associated with recrystallization

The initial development of small recrystallized grains is spatially associated with grain boundary and deformation band boundary bulging in the coarse deformed grains (Figs. 7a & b). The recrystallized grain sizes vary between different fault zones, but new grains averaging about 20–100 μm in diameter are typical. Recrystallized grains are polygonal and equant to slightly elongate, or occasionally irregularly shaped, with generally straight to gently curved grain boundaries (Figs. 7b & c). They show little optical evidence of deformation after treatment with the H_2O_2/NH_4OH etch, though they can contain broad, parallel-sided growth twins which may be gently bent. The acetic acid etch however reveals well-developed deformation substructures in many recrystallized grains (Fig. 7d). Others, particularly some of the more equant ones, apparently have no subgrain structure, or only a poorly developed one. This type of microstructure is typical of that expected during dynamic recrystallization, and is similar to the microstructure developed during high temperature steady-state dislocation creep in some metals (see Sellars 1978, Honeycombe & Pethen 1972) and many other minerals during dynamic recrystallization (Bell & Etheridge 1976, White 1977, Etheridge & Wilkie 1979, Weathers *et al.* 1979, Guillope & Poirier 1979, Cox *et al.* 1981, Christie & Ord 1981).

Both bulge nucleation and subgrain nucleation processes appear to have been important during dynamic recrystallization in chalcopyrite. At least in the initial stages of grain boundary and deformation band boundary recrystallization, the spatial association of recrystallized grains and regions of extensive grain boundary bulging, together with the fact that the diameters of new grains and associated bulges are similar, indicates that initial new grain generation involves a bulge nucleation mechanism. Subgrain structures are well developed in deformed grains at the commencement of boundary migration and recrystallization (Figs. 8a & b), and in

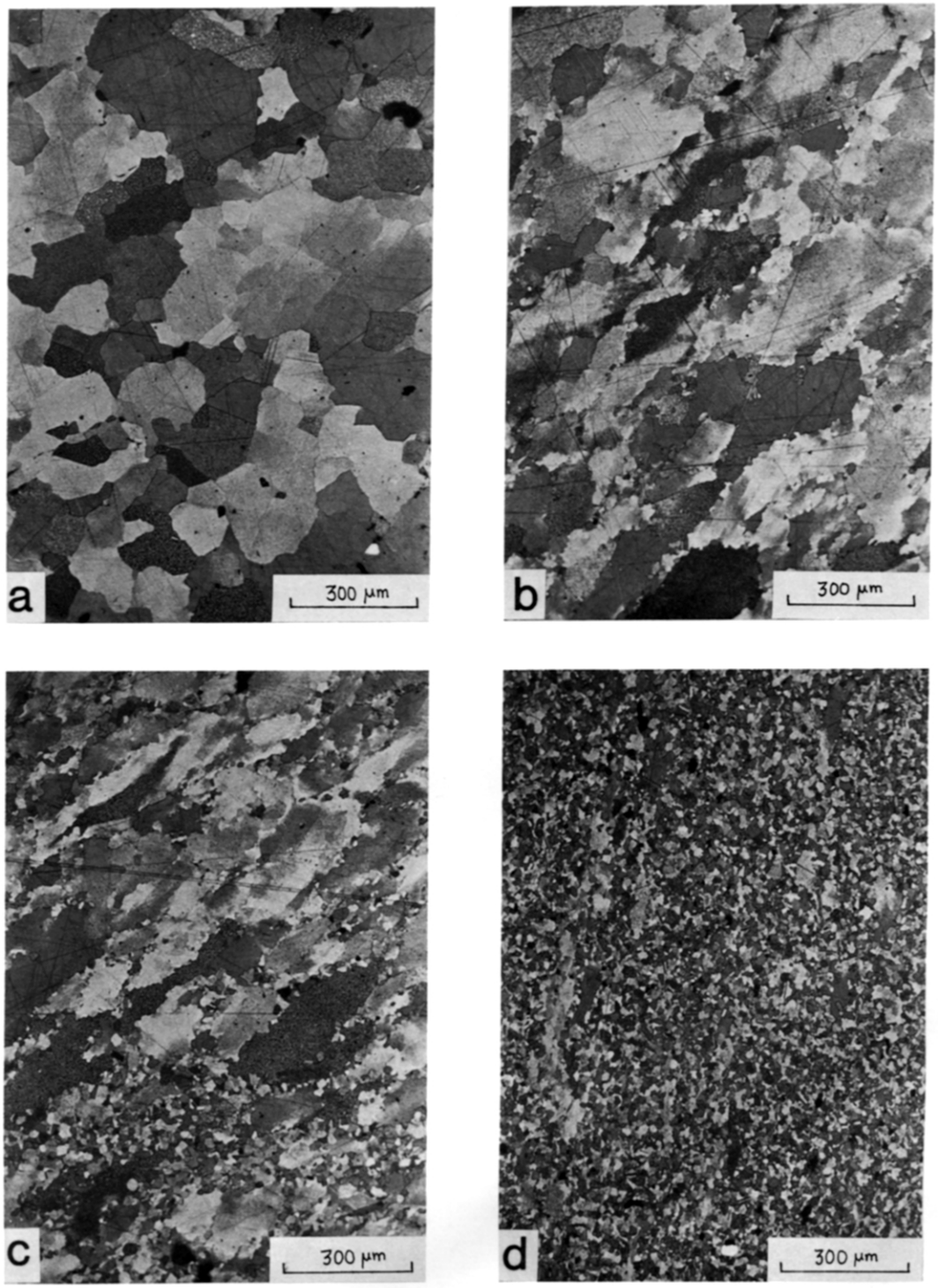

Fig. 2. Progressive microstructural transition with increasing strain in the shear zone illustrated in Fig. 1. NH_4OH/H_2O_2 etch. (a) Weakly deformed chalcopyrite at the margin of the shear zone. (b) Deformed, elongate chalcopyrite showing grain boundary migration, the early stages of grain boundary recrystallization, and the development of a subgrain structure. (c) Partly recrystallized chalcopyrite mylonite near the centre of the shear zone. (d) Extensively recrystallized chalcopyrite mylonite at the centre of the shear zone.

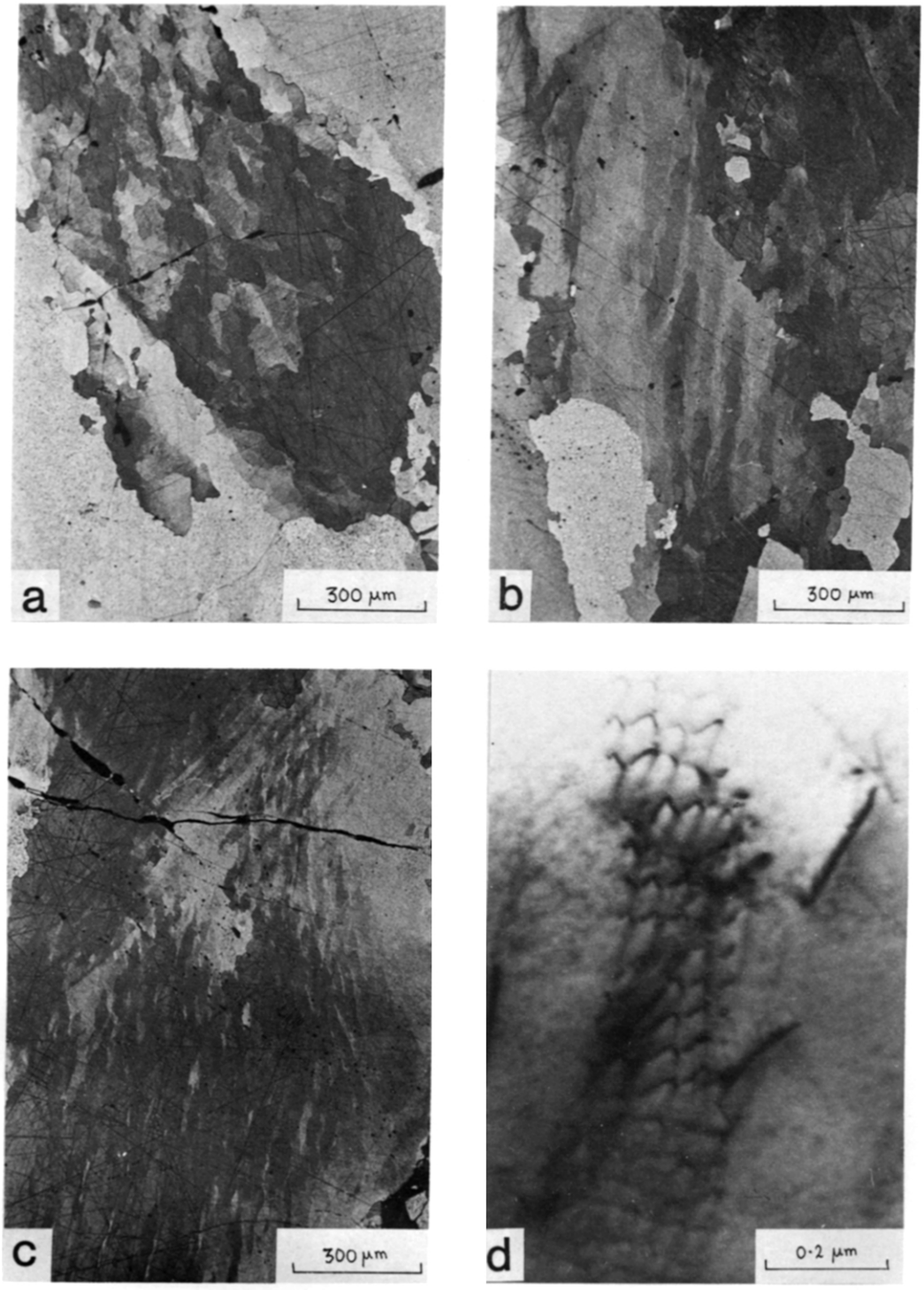

Fig. 3. Details of microstructures in coarse deformed grains in largely unrecrystallized chalcopyrite mylonites. (a) Equant to elongate subgrains in an elongate chalcopyrite grain. NH_4OH/H_2O_2 etch. (b) Deformation band structure. NH_4OH/H_2O_2 etch. (c) Two sets of deformation bands developed in an elongate grain. NH_4OH/H_2O_2 etch. (d) Well-ordered dislocation network forming a subgrain boundary. (TEM)

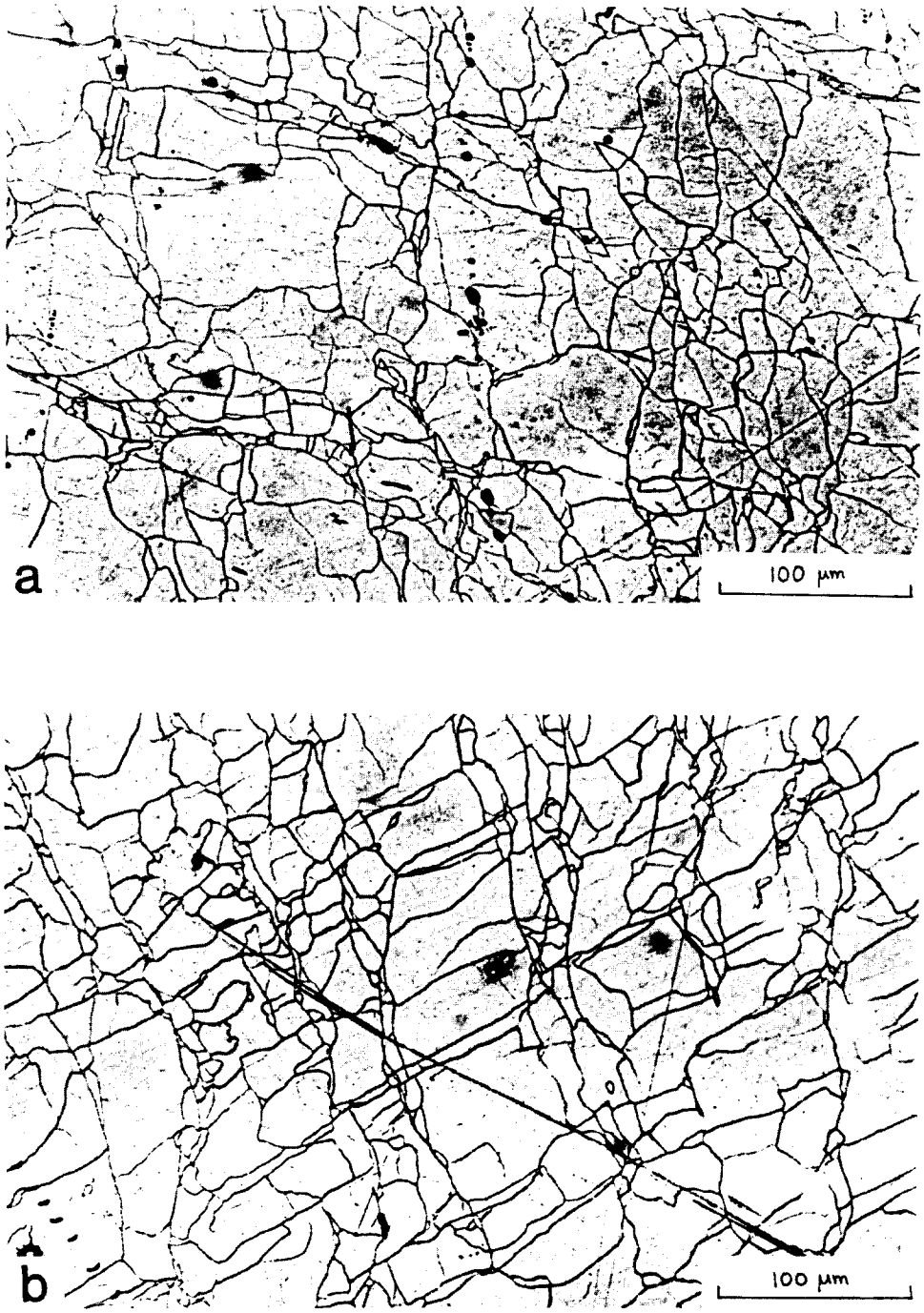

Fig. 4. Subgrain boundary structures in deformed chalcopyrite. Acetic acid etch. (a) Weakly oriented subgrain boundaries which enclose generally equant to irregularly shaped subgrains. (b) Highly oriented subgrain boundaries within one grain enclosing subgrains with equant to elongate shapes.

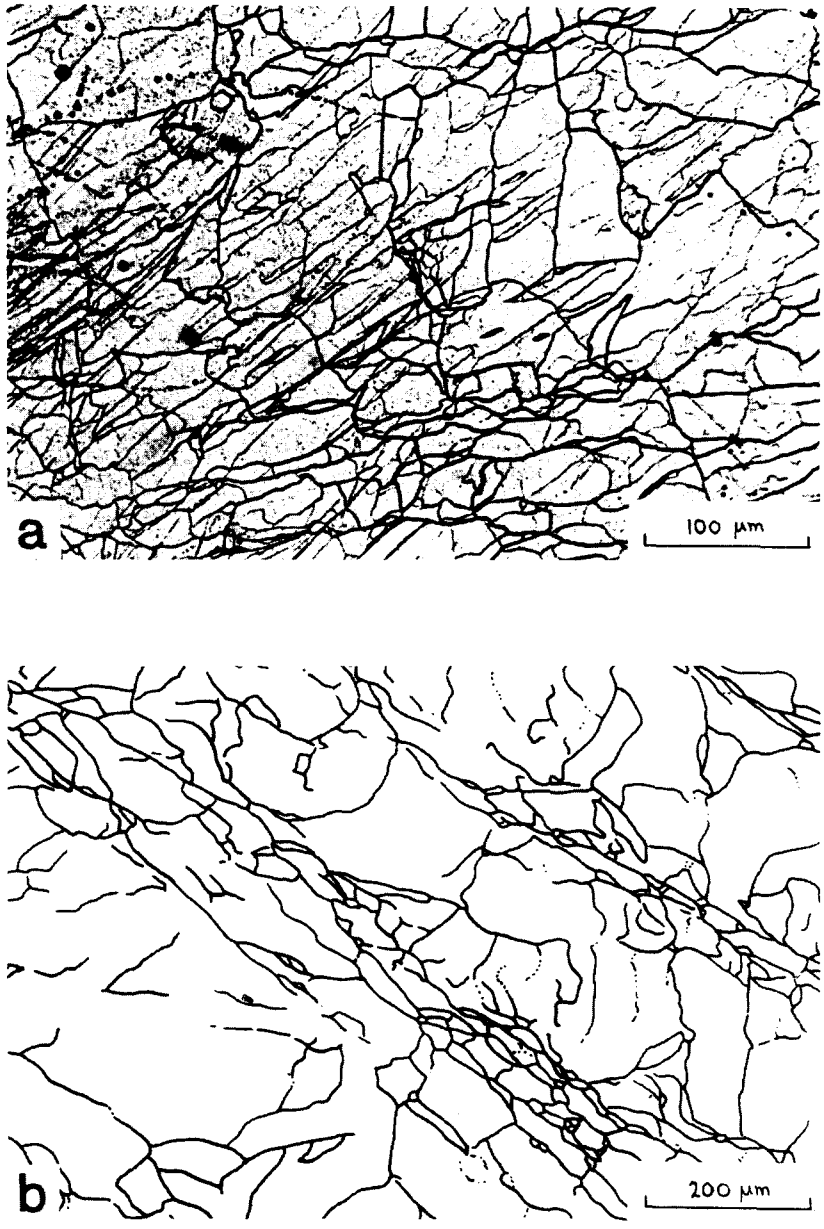

Fig. 5. (a) Elongate subgrain structure within a highly strained chalcopyrite grain. Note that between the heavily etched boundaries there are some highly oriented and more weakly etched boundaries. Acetic acid etch. (b) Highly oriented and closely spaced subgrain boundaries forming a deformation band boundary in a single chalcopyrite grain. Outside d.b.b. areas the subgrains have diameters an order of magnitude larger than within the d.b.b. areas, and are less well defined and more irregularly shaped. Traced from a micrograph of an acetic acid etched sample.

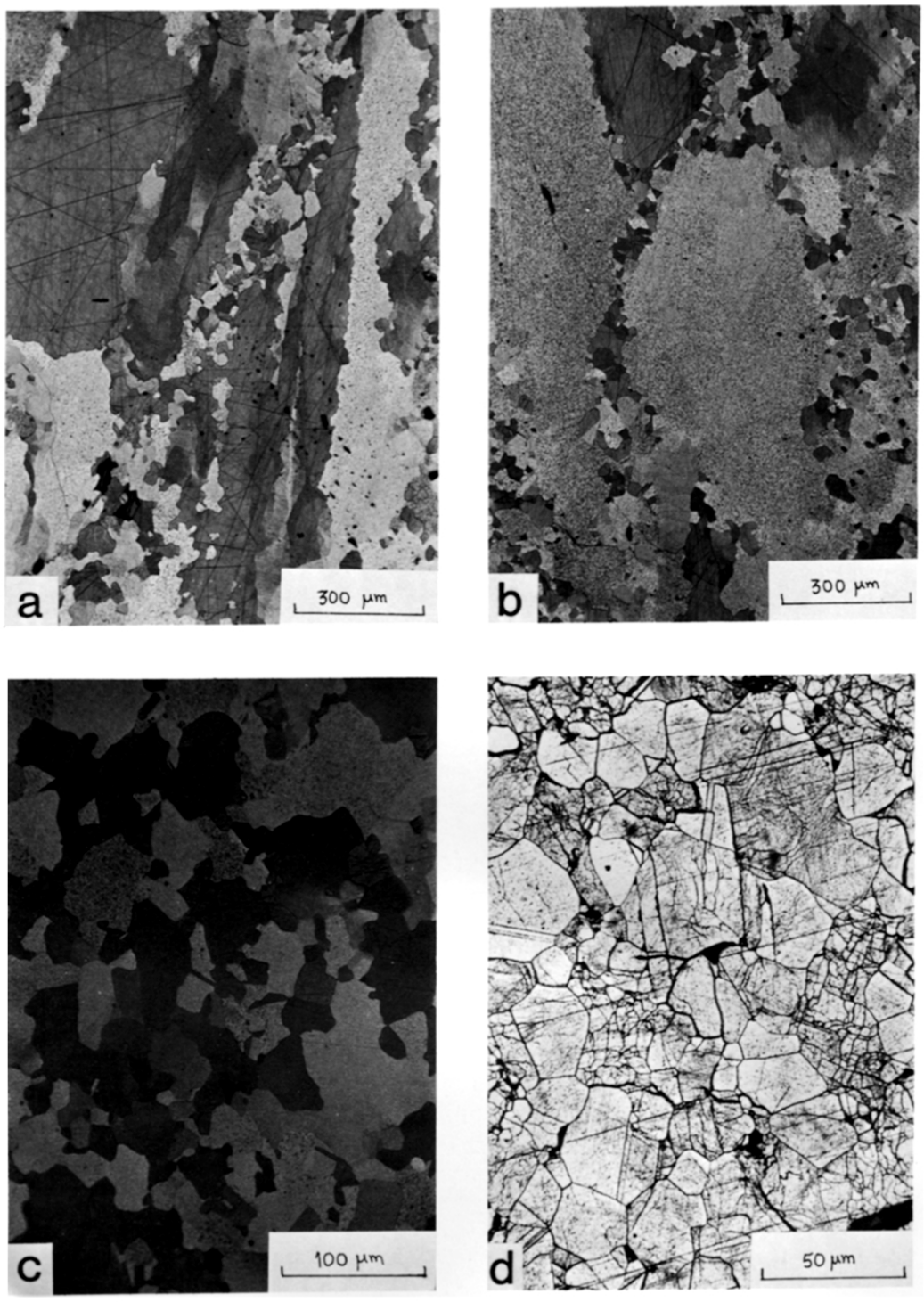

Fig. 7. (a) Elongate, deformed, and partly recrystallized grains showing extensive strain induced grain boundary and deformation-band boundary bulging. Small recrystallized grains have dimensions similar to those of the bulges. NH_4OH/H_2O_2 etch. (b) Equant polygonal to slightly elongate or irregularly shaped recrystallized grains developed at the grain boundaries of elongate deformed grains. NH_4OH/H_2O_2 etch. (c) Fine-grained recrystallized chalcopyrite grain aggregate. NH_4OH/H_2O_2 etch. (d) Detail of grain boundary and subgrain boundary configurations in a recrystallized chalcopyrite mylonite. Acetic acid etch.

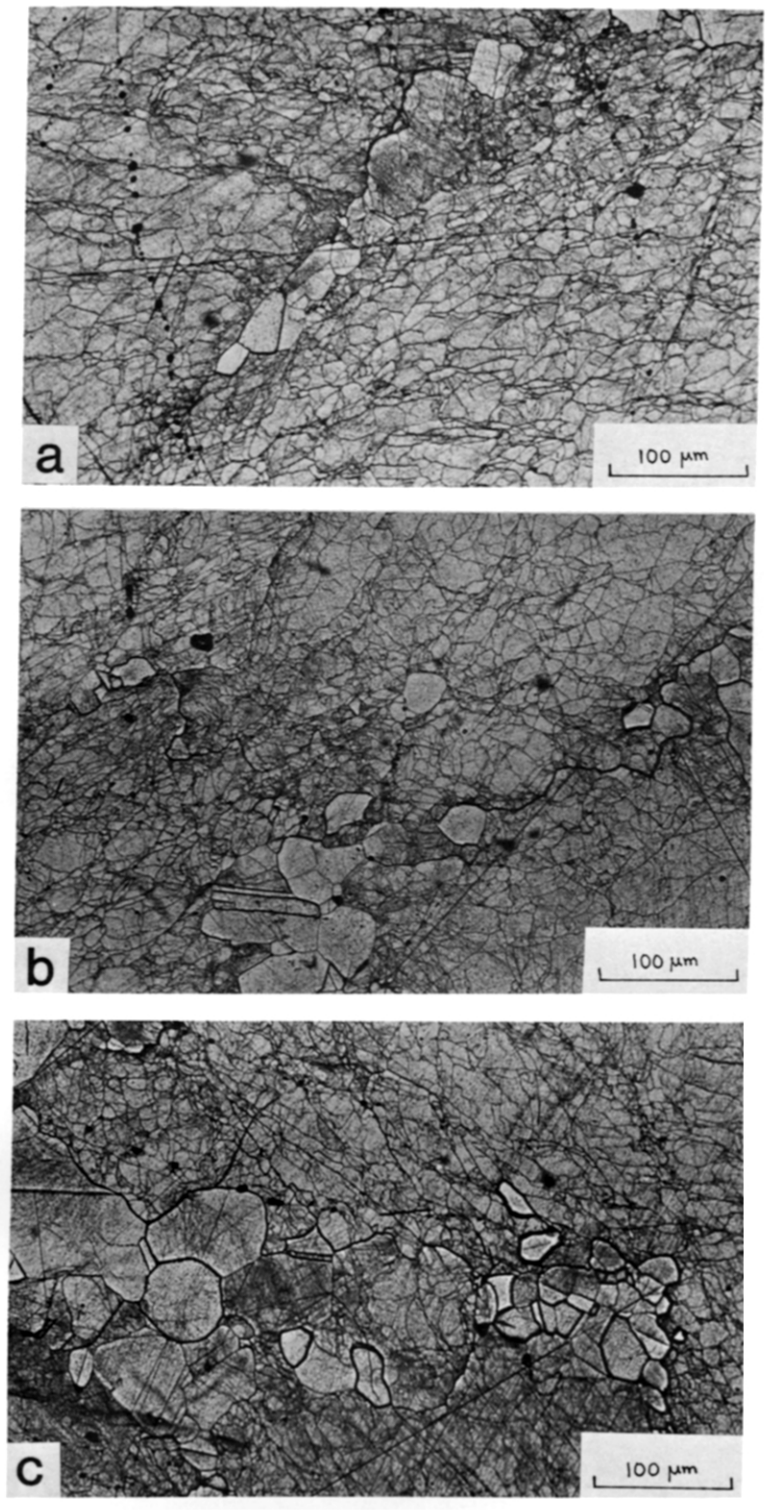

Fig. 8. Deformed grain and recrystallized grain relationships and subgrain boundary structures in regions of grain boundary recrystallization. Acetic acid etch. (a) Development of new polygonal grains, possibly by a bulge mechanism, in a deformation-band boundary region of a large host grain. Note similarity of recrystallized grain-size with subgrain size away from grain boundary regions. (b) The deeply etched host-grain boundary to the right is very lobate and associated with new grains having dimensions similar to those of adjacent subgrains. Coarser recrystallized grains in the lower part of the micrograph may have developed by a subgrain coalescence mechanism, or coalescence of new grains after recrystallization. (c) Very variable recrystallized grain size in a grain boundary region between two large deformed grains.

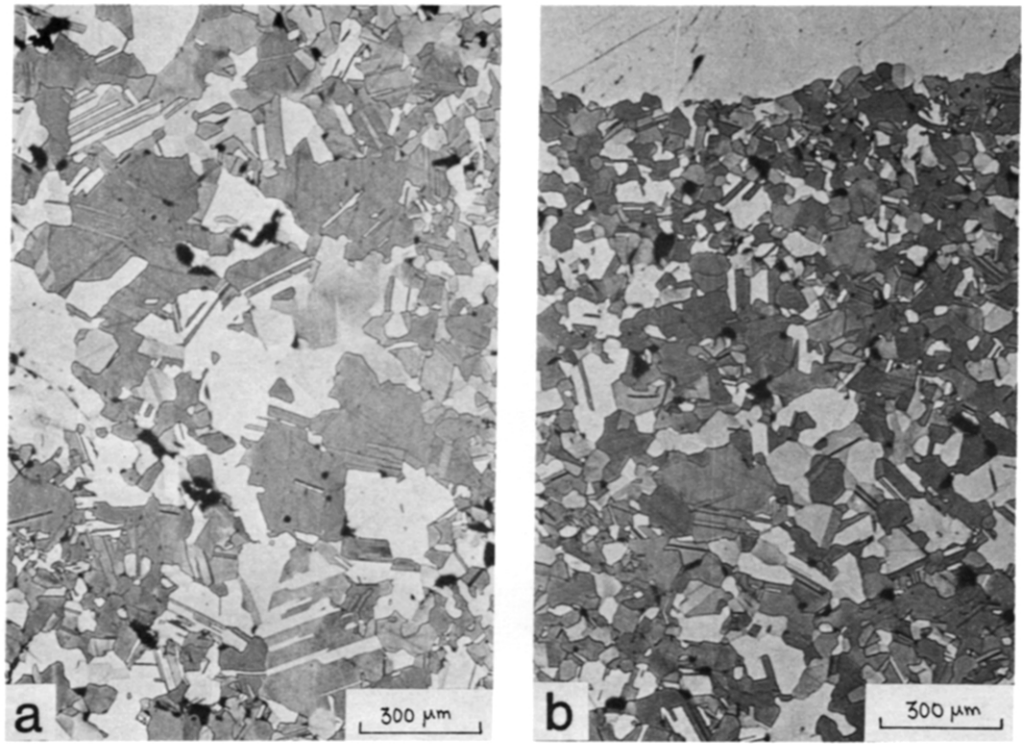

Fig. 9. (a) Recrystallized chalcopyrite mylonite containing a high growth twin incidence. NH_4OH/H_2O_2 etch. (b) Increasing grainsize of recrystallized chalcopyrite away from deformed host grain. NH_4OH/H_2O_2 etch.

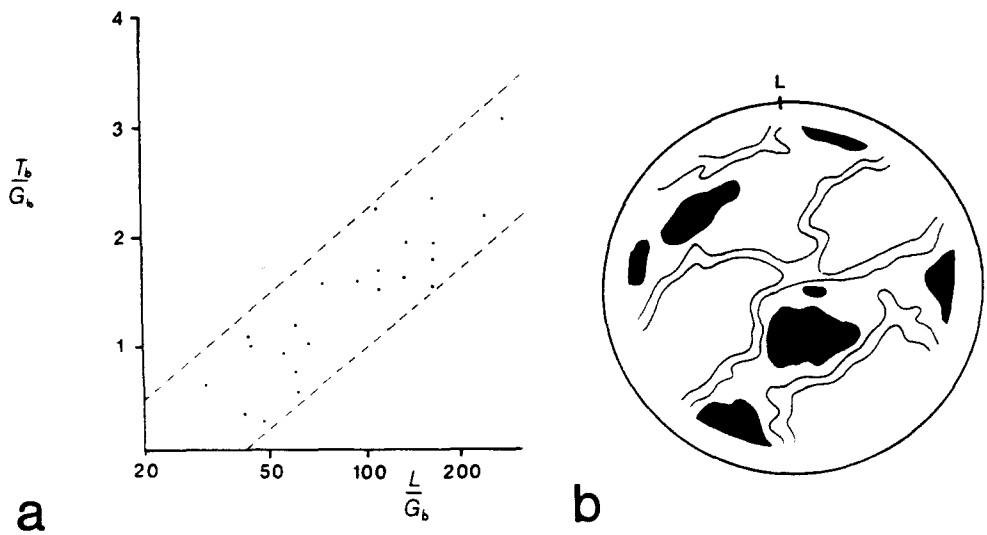

Fig. 10. (a) Relationship between within-grain twin boundary incidence (*Tb/Gb*) and average intercepted grain diameter (*L/Gb*) . *Tb* and *Gb* are respectively the number of twin boundaries and grain boundaries intercepted over a traverse of length *L*. (b) {112} pole figure for the largely recrystallized chalcopyrite mylonite shown in Fig. 9. Foliation defined by relict deformed grains is approximately parallel to the projection plane. The lineation (*L*) is indicated. Contour intervals at 1, 2 and 3 times uniform.

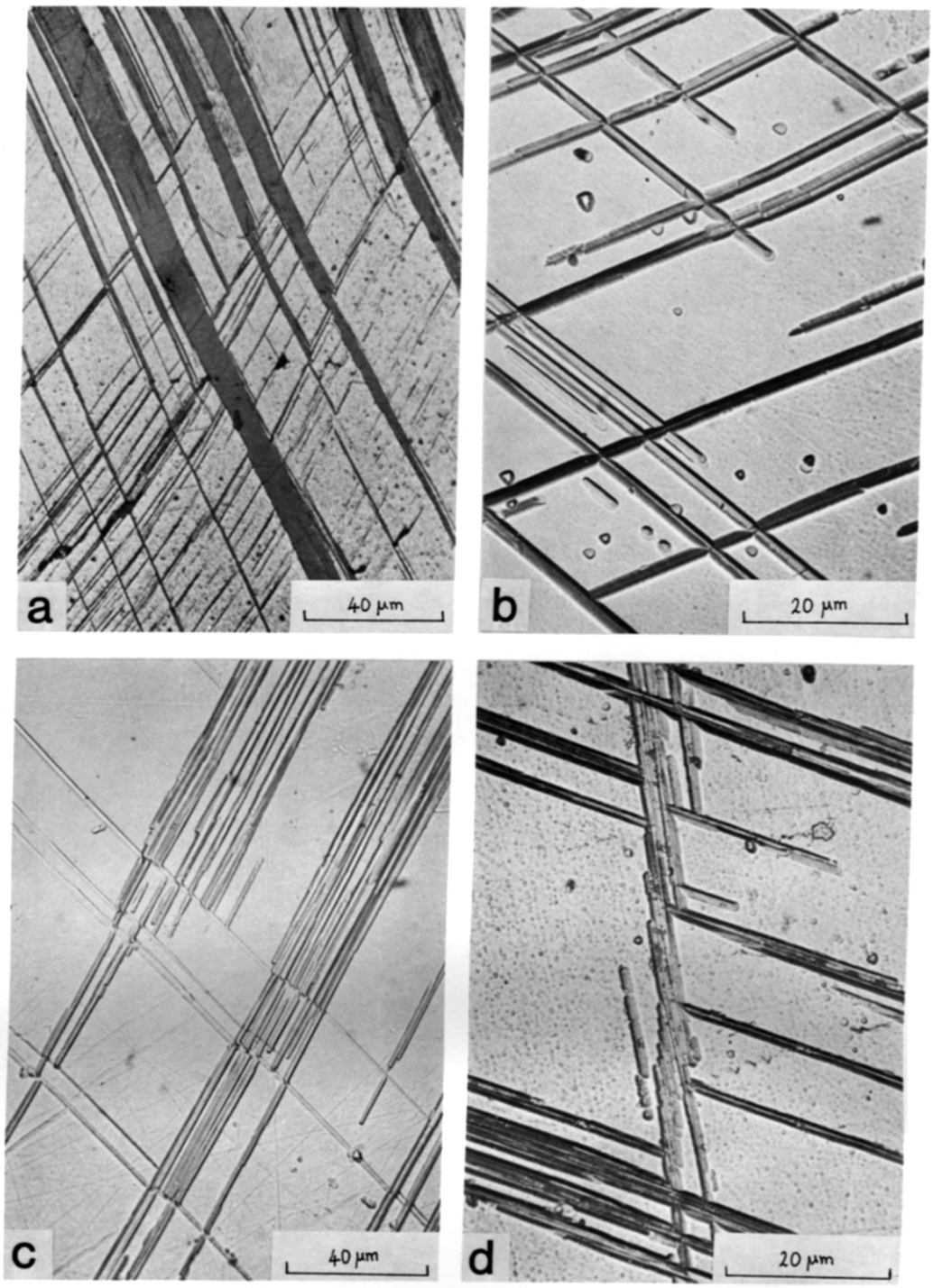

Fig. 11. Microstructures produced by deformation twinning in chalcopyrite. (a) Two sets of {112} deformation twins. NH_4OH/H_2O_2 etch. (b) Fine {112} deformation twins. Chromic acid etch. (c) Clustering of {112} deformation twins. Chromic acid etch. (d) En échelon arrays of deformation twins. Chromic acid etch.

some cases subgrain boundaries appear to be pinning bulges. New grains developed at the initial stages of grain boundary recrystallization have dimensions ranging from that of the first-order subgrain size up to several times the diameter of associated subgrains.

Once the original grain boundaries of old grains have been largely recrystallized grain boundary bulging is not so evident and subgrain nucleation mechanisms of recrystallization are probably more dominant. At the advanced stages of grain boundary recrystallization, and to some extent at the initial stages, etch colour changes indicating increased lattice rotation and subgrain misorientation adjacent to grain boundaries of deformed grains suggest that a subgrain rotation mechanism (Hobbs 1968, White 1973, 1976, 1977, Poirier & Nicolas 1975) has operated. The details of the transition from subgrains to recrystallized grains is unclear. However, in areas of advanced recrystallization, the stable recrystallized grain size is usually up to four or five times the first-order subgrain size in adjacent deformed grains (Fig. 8c), indicating that subgrain growth or coalescence may occur during recrystallization. In a few deformed grains adjacent to recrystallized regions, an intermediate stage in the recrystallization process may be represented by aggregates of several 'first-order' subgrains which are enclosed by roughly polygonal boundaries which are more deeply etched, and probably have a higher misorientation, than the usual subgrain. A possible recrystallization scenario in this case is that subgrain boundaries more widely spaced than the 'first-order' boundaries become more highly misoriented such that at some critical misorientation they become grain boundaries. Local migration of these boundaries is necessary to develop polygonal grain shapes. The lack of well developed subgrain structures in most new grains adjacent to deformed grains requires that the subgrain boundaries migrate and coalesce during the transition to a recrystallized grain.

Grain growth in a recrystallized chalcopyrite mylonite

A proportion of recrystallized grains in the chalcopyrite mylonites studied contain one or more broad, parallel-sided growth twins indicating that some grain-growth, albeit limited in most cases, can occur following nucleation (Fig. 8c). Continued cycles of dynamic recrystallization during steady-state creep are expected to maintain a fairly constant stress dependent recrystallized grain size and inhibit grain growth during deformation (Sah *et al.* 1974).

Fairly uniform recrystallized grain sizes, which are independent of strain in individual mylonite zones, together with the generally low growth twin incidence within individual grains, are taken to indicate that post-deformation annealing and grain growth are in most cases not very significant. However, there is an unusual example of a largely recrystallized microstructure in which the recrystallized grain size ranges from 30 to ~300 μm (Fig. 9). Variations in recrystallized grain size occur throughout the specimen, and define a weak grain size layering which is parallel to the grain elongation foliation defined by a few relict large deformed grains. In some areas there is a successive increase in the diameter of recrystallized grains away from the boundaries of deformed host grains (Fig. 9b), suggesting that significant grain growth has followed nucleation. Subgrain boundary etching reveals well-developed subgrain structures typical of high strain in the relict deformed grains and some of the smaller recrystallized grains. Very poorly developed, and generally coarser subgrain structures are present in the coarse recrystallized grains.

An analysis of the incidence of growth twins in the recrystallized fraction, as a function of grain diameter (Fig. 10a) reveals that the ratio of twin boundary incidence to that of grain boundary incidence increases with grain size. This is consistent with grains growing at the expense of neighbours by incorporating them into a twinned orientation rather than incorporating them into the growing grain's own orientation. This is in accordance with the Fullman–Fisher concept of grain growth (Fullman & Fisher 1951, Hu & Smith 1956) which considers that the presence of growth twins in certain grains lowers the total interfacial free energy compared with that of a grain structure not containing such twins. This grain growth mechanism is based on an equilibrium balance between interfacial energies, particularly on the large differences between the energy of a coherent twin interface and that of an ordinary high-angle boundary in some materials (Form *et al.* 1980).

The data indicate that in the example illustrated in Fig. 10(a), the new grain diameter upon nucleation has been around 15–30 μm, and that up to ten-fold grain growth has occurred in some areas by a twin coalescence mechanism.

Microstructures such as those illustrated in Fig. 9(b), where the earliest formed recrystallized grains (furthest from deformed relict host grains) have coarsened the most, suggest that the early formed recrystallized grains had a longer growth period than the younger ones. This suggests that coarsening was syntectonic rather than static, as in the latter case all the recrystallized fraction would be expected to coarsen approximately uniformly. To a large extent then, coarsening of the recrystallized fraction must be a consequence of boundary migration driven by reductions in grain boundary energy.

The usual poorly developed deformation substructures of the larger recrystallized grains indicate that they have been only weakly strained. This, and the fact that their subgrain diameters are typically larger than those of the finer recrystallized grains and the relict deformed old grains, suggests that grain growth may have occurred in low deviatoric stress domains undergoing less strain than surrounding areas. However, the development of dynamically coarsened grains may be related to the 'migration recrystallization' process described by Guillope & Poirier (1979). In this case, the lack of well-developed subgrain structures in the coarsened grains is consistent with grain boundary migration and grain growth proceeding at a rate faster than the development of subgrain structures. Why such rapid boundary migra-

tion and growth should take place in dynamically recrystallized grains is unclear. In NaCl, Guillope & Poirier (1979) showed that 'migration recrystallization' occurred only after a certain initial strain and at stresses and temperatures higher than those in which rotation recrystallization was dominant. The boundary energy of the recrystallized grains presumably provides a large part of the driving force for grain growth. In the case of the chalcopyrite mylonite, lattice coincidence relationships arising from the development of a strong lattice preferred orientation at high strain may be responsible for rapid boundary migration as has been observed in some metals (Aust & Rutter 1959).

The {112} pole figure for this type of largely recrystallized chalcopyrite mylonite (Fig. 10b) displays essentially the same features as that for the deformed but unrecrystallized chalcopyrite mylonites, a {112} plane lying close to the foliation and a $\langle 1\bar{1}0\rangle/\langle\bar{2}01\rangle$ direction, being close to the weak grain elongation lineation defined by relict deformed grains. However, there is a significant spread of {112} poles in girdles between the four dominant {112} maxima. This may reflect a fabric change brought about during grain growth.

MICROFABRICS PRODUCED BY DEFORMATION TWINNING AND BRITTLE FAILURE

Some coarse-grained and weakly deformed chalcopyrite in fault zone vein deposits has deformed by twin glide mechanisms as well as dislocation flow mechanisms.

The occurrence of deformation twinning in both experimentally and naturally deformed chalcopyrite has been well documented (Atkinson 1974, Kelly & Clark 1975, Roscoe 1975 in experimental studies; Shadlun 1953, Ramdohr 1969, Richards 1966 in naturally deformed chalcopyrite). Kelly & Clark (1975) determined that deformation twinning occurs in {112} orientations. This is analogous to the development of (111) deformation twins in face-centred cubic metals and sphalerite.

The abundantly developed deformation twins illustrated in Fig. 11 are similar to those produced in experimental studies, and can be distinguished optically from the broad parallel-sided or stepped and bluntly terminated growth twins on the basis of their very fine, tapering and discontinuous habit which is best revealed by the NH_4OH/H_2O_2 etch. The deformation twins are up to several millimetres long and commonly extend only part of the way across a grain. They are usually less than 5 μm thick, and seldom exceed 20 μm in thickness. One to three sets of such twins may be present in grains, though rarely the maximum number of four sets of {112} twins has been observed.

Twin abundance has been found to be very variable, but may reach up to ten twins per 50 μm. The individual twins in some cases converge, and small tapering extensions which branch off a larger twin are commonly developed. Twins of one set may also be present in periodic clusters (Fig. 11c) in which several twins are present over an interval of 10–15 μm, with a gap of 50–100 μm separating adjacent clusters. En échelon arrays of twins (Fig. 11d) are also developed.

In a few cases, chalcopyrite from the fault zone deposits has deformed by intragranular and transgranular shear microfracturing as well as by deformation twinning and dislocation flow. Apparent displacements of up to 50 μm across microfractures are indicated by offsets of pre-fracture {112} deformation twins. Such microfractures are usually sharply defined and planar to gently curved. Most shear microfractures are healed, and in a few cases associated with planar zones of fine (10–20 μm) polygonal chalcopyrite grains which appear to occur along the larger microfractures as well as patchily replacing some coarse twinned chalcopyrite adjacent to parts of the smaller shear microfractures. In some cases the fine polygonal chalcopyrite appears to be infilling extension microfracture sites.

DISCUSSION AND CONCLUSIONS

Much of the chalcopyrite in vein deposits within fault zones at Mt. Lyell has been deformed by dislocation flow processes with the accompanying development of strong lattice preferred orientations which are consistent with the operation of $\{112\}\langle 1\bar{1}0\rangle/\langle\bar{2}01\rangle$ dislocation glide during simple shearing deformation. In the tetragonal chalcopyrite structure, metal atoms are arranged in a face-centred cubic lattice such that Fe and Cu atoms alternate in the [100] direction. Each metal atom is co-ordinated by a tetrahedron of S atoms; thus the S atoms are arranged in layers stacked in cubic close packing. These layers are parallel to {112} planes in the chalcopyrite tetragonal cell. On structural grounds then, {112} glide in $\langle 1\bar{1}0\rangle$ or $\langle\bar{2}01\rangle$ directions is expected, and appears to be the easiest slip system. This is analogous to the common $\{111\}\langle 1\bar{1}0\rangle$ dislocation glide in f.c.c. metals and sphalerite.

As a result of deformation experiments, Mügge (1920), Buerger (1928) and Kelly & Clark (1975) determined that the {112} planes are the main glide planes in chalcopyrite at room temperture. Kelly & Clark (1975) could not definitely establish the glide directions, but Lang (1968) in room temperature tests produced crystallographic preferred orientations consistent with glide in the close-packed $\langle 1\bar{1}0\rangle$ and $\langle\bar{2}01\rangle$ directions. At geological strain rates and low-grade metamorphic temperatures the major operative glide system in chalcopyrite thus appears to be the same as that operative at room temperature and laboratory strain rates. In the naturally deformed chalcopyrite however, the development of microstructures indicative of dynamic recovery and recrystallization indicate that dislocation climb, as well as glide, has been operative.

Significant static recovery and annealing recrystallization in the fault zone chalcopyrite is considered unlikely as free dislocation densities during dislocation creep would have been low. Accordingly, grains would have

had low internal strain energies. Similarly, grain and subgrain boundaries are expected to have had low energy configurations. The preservation of well-developed deformation substructures in both deformed and recrystallized grains, and particularly the occurrence of uniform recrystallized grain sizes within most samples, irrespective of strain, argues against significant static strain-induced recovery, grain boundary migration, and recrystallization being important in the development of the microstructure. Dynamic coarsening of recrystallized grains has been demonstrated in one case, but this is ascribed to either boundary migration driven by a lowering of interfacial free energies in low deviatoric stress domains, or alternatively the phenomenon may be related to 'migration recrystallization' (Guillope & Poirier 1979). Grain growth driven by reductions in interfacial free energy is thermally activated and may also depend on the fluid environment (Tullis & Yund 1982). Thus if a high temperature regime or suitable chemical environment outlasts the deformation history, some static grain growth may be expected.

The chalcopyrite that has been deformed by mechanical twinning also usually shows evidence of slight dislocation flow deformation. Time relations between the operation of dislocation creep and twinning are generally uncertain, but the intense development of thin deformation twins at sites of marked lattice bending in some samples suggests that the two processes were partly synchronous.

The development of mechanical twinning in many materials is relatively temperature insensitive (Tullis 1980) but strongly stress dependent (Reed-Hill 1964). These features, and the fact that the critical resolved shear stress for dislocation glide decreases with increasing temperature, mean that twinning is more active at higher stresses and lower temperatures than dislocation creep (Reed-Hill 1964, Turner 1964). Thus for chalcopyrite specimens in which twin glide has been the dominant deformation mechanism, deformation has probably occurred late during the fault history in a waning thermal regime, and possibly at relatively high deviatoric stress levels.

In samples in which brittle failure has occurred, microfracturing post-dates deformation twinning and indicates deformation at either higher stress/lower temperature, or possibly by hydraulic fracture during periods of local high fluid pressure in the fault zones.

The results of this study have wider application to the interpretation of deformation microfabrics in other minerals, particularly silicates. The use of etching techniques to reveal subgrain structures developed in deformed and recrystallized grains has provided useful information on the processes involved in dynamic recrystallization. It is clear that several mechanisms have been important in the development of the recrystallized microstructure. At least in the early stages of grain boundary recrystallization, a bulge nucleation mechanism has operated. There is also evidence, particularly at higher strains where host grain boundaries are largely recrystallized, that recrystallization results from progressive rotation of subgrains. Such a change in recrystallization mechanisms with increasing strain has been well documented in pyroxene (Etheridge & Kirby in press).

Typically the stable recrystallized grain size is somewhat larger than the subgrain size, and recrystallized grains themselves are large enough to contain well-developed subgrain structures. The details of the transition from a strained subgrain structure to virtually unstrained recrystallized grains remain unclear. In some cases at least, subgrain coalescence or growth, as well as rotation, must be involved in the recrystallization process.

Coalescence and growth of recrystallized grains has been demonstrated to occur to a small extent in most of the chalcopyrite mylonites studied, though extensive dynamic coarsening has been demonstrated in one example. The reasons for such coarsening are not completely understood, but the recognition of grain growth in dynamically recrystallized minerals is important in the interpretation of completely recrystallized materials, especially when used as stress/grain size indicators.

The similarity in deformation mechanisms and microstructures of silicate minerals and sulphides such as chalcopyrite suggests that some sulphides may be suitable experimental silicate analogues useful in studying the influence of environmental variables on mechanical behaviour and microstructural development, particularly dynamic recrystallization processes, at relatively low deviatoric stresses and moderate homologous temperatures.

Acknowledgements—One of us (S.F.C.) wishes to acknowledge the financial support of a Commonwealth Postgraduate Research Award, a C.S.I.R.O. Postdoctoral Studentship, and a Queen Elizabeth II Fellowship during various stages of the study. Presentation of this paper at the International Conference on Planar and Linear Fabrics of Deformed Rocks in Zürich (1982) was aided by the generous support of a travel grant from the Ian Potter Foundation. We would like to thank Bruce Hobbs, Heinrich Siemes and Alison Ord for stimulating discussion and comments on the manuscript.

The management of the Mt. Lyell Mining and Railway Co. Ltd is thanked for ready access to their mines and for support in the field. X-ray fabric studies were conducted at the B.H.P. Melbourne Research Laboratories with the generous assistance of Dr Pat Wright and Phillip Stevens.

REFERENCES

Atkinson, B. K. 1974. Experimental deformation of polycrystalline galena, chalcopyrite, and pyrrhotite. *Trans. Inst. Min. Metall.* **B83**, B19–B28.

Aust, K. T. & Rutter, J. W. 1959. Grain boundary migration in high purity lead and lead–tin alloys. *Trans. Metall. Soc. AIME* **215**, 119–127.

Bell, T. H. & Etheridge, M. A. 1976. The deformation and recrystallization of quartz in a mylonite zone, central Australia. *Tectonophysics* **32**, 238–267.

Buerger, M. J. 1928. The plastic deformation of ore minerals, a preliminary investigation: galena, sphalerite, chalcopyrite, pyrrhotite, and pyrite. *Am. Miner.* **13**, 1–17, 35–51.

Chervyakovskii, G. F. 1952. Experiments on the recrystallization of sulphide minerals. *Dokl. Akad. Nauk. S.S.S.R.* **83**, 737–738.

Christie, J. M. & Ord, A. 1980. Flow stress from microstructures of mylonites: example and current assessment. *J. geophys. Res.* **85**, 6253–6262.

Cox, S. F. 1981. The stratigraphic and structural setting of the Mt. Lyell volcanic-hosted sulfide deposits. *Econ. Geol.* **76**, 231–245.

Cox, S. F., Etheridge, M. A. & Hobbs, B. E. 1981. The experimental ductile deformation of polycrystalline and single crystal pyrite. *Econ. Geol.* **76**, 2105–2117.

Deer, W. A., Howie, R. A. & Zussman, J. 1969. *An Introduction to the Rock-forming Minerals*. Longmans, London.

Etheridge, M. A. & Kirby, S. H. in press. Experimental deformation of rock-forming pyroxenes: recrystallization mechanisms and preferred orientation development. *Tectonophysics*.

Etheridge, M. A. & Wilkie, J. C. 1979. Grainsize reduction, grain boundary sliding, and the flow strength of mylonites. *Tectonophysics* **58**, 159–178.

Form, W., Gindraux, G. & Mlyncar, V. 1980. Density of annealing twins. *Met. Sci.* **14**, 16–20.

Fullman, R. L. & Fisher, J. C. 1951. Formation of annealing twins during grain growth. *J. appl. Phys.* **22**, 1350–1355.

Gill, J. E. 1969. Experimental deformation and annealing of sulfides, and the interpretation of ore textures. *Econ. Geol.* **64**, 500–508.

Guillope, M. & Poirier, J. P. 1979. Dynamic recrystallization during creep of single-crystalline halite: an experimental study. *J. geophys. Res.* **84**, 5557–5567.

Hobbs, B. E. 1968. Recrystallization of single crystals of quartz. *Tectonophysics* **6**, 353–401.

Honeycombe, R. W. K. & Pethen, R. W. 1972. Dynamic recrystallization. *J. Less-Common Metals* **28**, 201–212.

Hu, H. & Smith, C. S. 1956. The formation of low energy interfaces during grain growth in alpha and alpha–beta brasses. *Acta Metall.* **4**, 638–646.

Jonas, J. J., McQueen, H. J. & Wong, W. A. 1968. Dynamic recovery during the extrusion of aluminium. *Iron and Steel Inst. Publ.* **108**, 49–59.

Kelly, W. C. & Clark, B. R. 1975. Sulfide deformation studies—III. Experimental deformation of chalcopyrite to 2000 bars and 500°C. *Econ. Geol.* **70**, 431–453.

Korn, D. 1933. Ein deformiertes Flusspart–Quartz–Kupferkies gefüge aus einer mittelschwedischen Sulfidlagerstätte. *Neues Jb. Mineral. Geol. Paläont. Beil. Bd.* **A66**, 433–459.

Kohlstedt, D. L. & Weathers, M. S. 1980. Deformation-induced microstructures, paleopiezometers, and differential stresses in deeply eroded fault zones. *J. geophys. Res.* **85**, 6269–6285.

Krishnamurthy, P. 1967. Experimental deformation of sulphide ores. Unpublished M.Sc. thesis. McGill University, Montreal.

Lang, H. 1968. Stauchversuche mit polykrystallinen Kupferkiesen und derem Ergebnisse unter besonderer Berucksichtigung der Gefugeregelung. Dr. Ing. Diss. Rheinisch Westfällischen T.H., Aachen.

Mügge, O. 1920. Über translationen am Schwefel, Periclas und Kupferkies und einfache Schiebungen am Bournonit, Pyrargyrit, Kupferglanz und Silberkupferglanz. *Neues Jb. Mineral. Geol. Paläont.* **1920**, 24–54.

Newhouse, W. H. & Flaherty, G. F. 1930. The texture and origin of some banded or schistose sulphide ores. *Econ. Geol.* **25**, 600–620.

Poirier, J. P. 1972. High temperature creep of single crystalline sodium chloride. *Phil. Mag.* **26**, 713–725.

Poirier, J. P. & Nicolas, A. 1975. Deformation induced recrystallization due to progressive misorientation of subgrains, with special reference to mantle peridotites. *J. Geol.* **83**, 707–720.

Ramdohr, P. 1969. *The Ore Minerals and their Intergrowths*. Pergamon, Oxford.

Ramsay, J. G. 1967. *Folding and Fracturing of Rocks*. McGraw-Hill, New York.

Reed-Hill, R. E. 1964. Role of plastic deformation of a polycrystalline anisotropic metal. In: *Conference on Deformation Twinning* (edited by Reed-Hill, R. E., Hirth, J. P. & Rogers, H. C.). Gordon and Breach, New York, 295–320.

Reid, K. O. 1975. Mount Lyell copper deposits. In: *Economic Geology of Australia and Papua-New Guinea*, 1. *Metals* (edited by Knight, C. L.). Australasian Inst. Mining Metallurgy, Monogr. 5, 604–619.

Richards, S. M. 1966. Mineragraphy of fault-zone sulphides, Broken Hill, N.S.W. C.S.I.R.O. Mineragraphic Investigations, Tech. Paper 5, 1–24.

Richardson, G. L., Sellars, S. M. & Tegart, W. J. McG. 1966. Recrystallization during creep of nickel. *Acta Metall.* **14**, 1225–1236.

Roberts, W. M. B. 1965. Recrystallization and remobilization of sulfides at 2000 atmospheres and the temperature range 50–145°. *Econ. Geol.* **60**, 168–171.

Roscoe, W. E. 1975. Experimental deformation of natural chalcopyrite at temperatures up to 300°C over the strain rate range 10^{-2} to 10^{-6} sec^{-1}. *Econ. Geol.* **70**, 454–472.

Sah, J. P., Richardson, G. P. & Sellars, C. M. 1974. Grainsize effects during dynamic recrystallization of nickel. *J. Met. Sci.* **8**, 325–331.

Sellars, C. M. 1978. Recrystallization of metals during hot deformation. *Phil. Trans. R. Soc.* **A288**, 147–198.

Shadlun, T. N. 1953. The change in the structure of grains of chalcopyrite subjected to the influence of dynamic factors. *Mineral. Sbornik [Lvov] Geol. Ser.* **7**, 75–80.

Takeuchi, S. & Argon, A. S. 1976. Steady state creep of single-phase crystalline matter at high temperatures. *J. Mater. Sci.* **11**, 1542–1566.

Tullis, J. & Yund, R. A. 1982. Grain growth kinetics of quartz and calcite aggregates. *J. Geol.* **90**, 301–318.

Tullis, T. E. 1980. The use of mechanical twinning in minerals as a measure of shear stress magnitude. *J. geophys. Res.* **85**, 6263–6268.

Turner, F. J. 1964. Some geometric aspects of experimentally induced twinning in minerals. In: *Conference on Deformation Twinning* (edited by Reed-Hill, R. E., Hirth, J. P. & Rogers, H. C.). Gordon and Breach, New York, 156–176.

Weathers, M. S., Cooper, R. F., Kohlstedt, D. L. & Bird, J. M. 1979. Differential stress determined from deformation-induced microstructures of the Moine Thrust zone. *J. geophys. Res.* **84**, 7495–7509.

White, S. 1973. Syntectonic recrystallization and texture development in quartz. *Nature, Lond.* **244**, 276–278.

White, S. 1976. The effect of strain on the microstructures, fabrics, and deformation mechanisms in quartzites. *Phil. Trans. R. Soc.* **A283**, 69–86.

White, S. 1977. Geological significance of recovery and recrystallization processes in quartz. *Tectonophysics* **39**, 143–170.

White, S. 1979. Grain and sub-grain size variations across a mylonite zone. *Contr. Miner. Petrol.* **70**, 193–202.

Zeuch, D. H. 1980. The Dislocation Substructure of Experimentally Deformed Synthetic Dunite. Ph.D. thesis, University of California, Davis, University Microfilms International, Ann Arbor.